P, Sb and Sn Ion Implantation with Laser Melt-LPC (Liquid Phase Crystallization) for High Activation n+ Ultra Shallow Junction in Ge Epilayer and Surface Strain-Ge Formation for Mobility Enhancement

John Borland, Joshua Herman[1], Steve Novak[1], Hiroshi Onoda[2], Yoshiki Nakashima[2], Karim Huet[3], Walt Johnson[4] and Abhijeet Joshi[5]

J.O.B. Technologies
Aiea, Hawaii, 96701, USA
E-mail: JohnOBorland@aol.com
[1] College of Nanoscale Science and Engineering, SUNY Polytechnic Institute, Albany, New York, 12203, USA
[2]Nissin Ion Equipment Company, 575, Kuze-Tonoshiro-Cho, Minami-Ku, Kyoto, 601-8205, Japan
[3]LASSE, Screen Semiconductor Solutions Co., Ltd, 14-38 rue Alexandre, 92230 Gennevilliers, France
[4]KLA-Tencor, 3 Technology Dr., Milpitas, CA, 95035, USA
[5]Active Layer Parametrics, 417 and a Half Veteran Ave, Los Angeles, CA, 90024, USA

1. Introduction

High mobility Ge or SiGe FinFET channel material is expected to be used starting at the 10nm or 7nm technology node. One major issue for Ge NMOS is the difficulty in achieving both n+ ultra-shallow junction (USJ) and high dopant activation. Implanted P, As and Sb n+ dopant activation in Ge using traditional RTA annealing increases with temperature as reported by Borland and Konkola [1] reaching saturation above 875°C. To prevent rapid diffusion of n+ dopant in Ge and achieve USJ, the RTA annealing temperature must be kept below 600°C but this reduces dopant activation level by 70% to low-E19/cm^3 as reported by Lee et al. [2]. The best n+ dopant activation is right at the melting point of Ge at 937°C and rapid n+ liquid phase diffusion to the liquid/solid interface occurs so the n+ junction depth is determined by the Ge layer thickness [1]. As the temperature exceeds 937°C, Si intermixing occurs forming a SiGe alloy degrading both mobility and n+ dopant activation level [1]. The solution is to use rapid and controlled Ge melt depth without Si intermixing to define the n+ junction depth in Ge. An example of melt depth controlled n+ junction in Ge using laser melt annealing was reported by Mazzocchi et al. [3] achieving P dopant activation level >1E20/cm^3. Thareja et al. [4] reported higher n+ activation for Sb compared to P and As using laser melt to control junction depth and defects for low leakage achieving Sb activation up to 4E20/cm^3 with As and P both at 2E20/cm^3.

The traditional method to form high mobility Ge and SiGe channel material is by CVD epitaxial deposition with varying surface mobility. Recently Borland et al [5,6] reported on an alternative method using amorphous Ge deposition by plasma and beam-line implantation followed by Ge-LPC (liquid phase crystallization) using laser melt annealing to form strain-SiGe and strain-Ge layers within the top few hundred angstroms of the Si surface thereby improving hole and electron mobility by 4x and 2x respectively. Therefore we will also report on our study to induce compressive or tensile surface strain-Ge in Ge-epilayer by Sn ion implantation.

2. Experimentation

We used 70nm undoped Ge epilayers with SiGe buffer layer on 300mm Si P(100) wafers provided by CNSE. Nissin performed half wafer Sn implants at 10keV/5E15 (~10% GeSn) to create a shallow amorphous layer 30nm deep. Then full wafer P implant at 4keV/5E15 or Sb implant at 11keV/5E15. The wafers were annealed using a 308nm Excimer laser annealer by LASSE (LT-3000) with varying energy density levels from 0.6J/cm^2 to 1.6J/cm^2 in the annealing pattern shown in Fig.1.

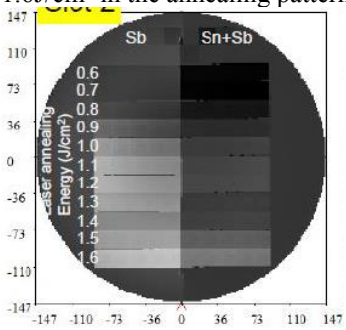

Fig.1: TW wafer map showing laser anneal regions.

3. Results

Dopant Activation by Rs 4PP

We used non-penetrating Hx 4 point probe by KLA-Tencor for the Rs sheet resistance measurements

shown in Fig.2. The Sn implant introduces acceptor level defects as reported by Zaima et al. [7] increasing Rs for the non-annealed Sn+Sb region by 3x from 4.7kΩ/□ to 10.8KΩ/□ and Sn+P region by 7x from 11KΩ/□ to 86KΩ/□. Sn+Sb required laser energy density >0.8J/cm^2 while Sn+P >1.0J/cm^2 to anneal out these acceptor defect levels. Note a slight rise in Rs for Sn+Sb implants >1.4J/cm^2 laser anneal. P Rs saturates at 60Ω/□ while Sb saturates 36% lower at 38Ω/□ when the laser melt depth exceeds the as implanted n+ junction depth.

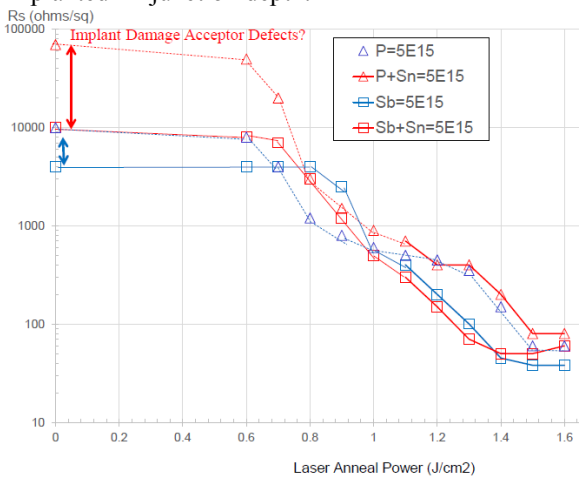

Fig.2: Hx-4PP Rs sheet resistance for various laser annealing conditions.

SIMS Depth Profiles

The as implanted unannealed P, Sn+P, Sb and Sn+Sb SIMS profiles provided by CNSE are shown in Fig.3. Considerable P implant channeling in Ge was detected by SIMS with a 1E19/cm^3 defined n+ Xj of 40.0nm compared to Sb with an Xj of 26nm. With the half wafer Sn implant first, the P channeling for the Sn+P implant region is eliminated but produces a deeper profile with less surface dopant pile-up and the same Xj of 40nm as does the Sn+Sb implant with an Sb Xj of 40nm. Note that the Sb profile shows no surface pile-up for the Sn+Sb implanted region but rather a well-defined retrograde Sb profile.

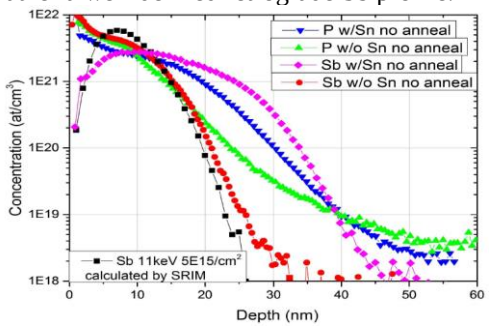

Fig.3: No anneal region SIMS profile showing channeling and non-channeling n+ profiles.

The laser annealing profiles for P only implants are shown in Fig.4. At 1.0J/cm^2 the melt depth was <10nm but at 1.4J/cm^2 it clearly was 25nm forming a box-like profile however, all the n+ junction depths (Xj) remained at 45nm.

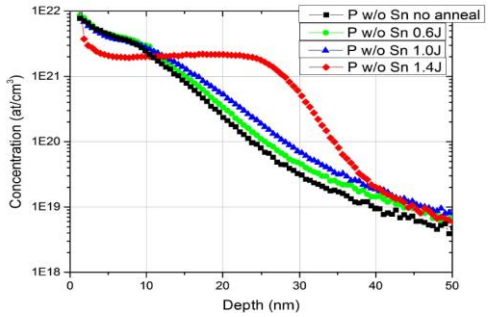

Fig.4: P SIMS profiles for 0.0, 0.6, 1.0 and 1.4J/cm^2 laser anneal conditions.

Results for the Sn+P laser anneals are shown in Fig.5 with n+ junction depth of 45nm for 1.0 and 1.4J/cm^2 but increases to 80nm for 1.5J/cm^2. The melt depth P profiles are similar to the non-Sn implanted region but the melt depth jumps from 25nm at 1.4J/cm^2 to 65nm at 1.5J/cm^2. The Sn-SIMS profiles are shown in Fig.6 and about a 10x drop in Sn areal density to 4.6E14/cm^2 occurred with the 1.4J/cm^2 anneal (melt depth of 38nm and Sn level of 3E20/cm^3) and then recovers to 5.2E15/cm^2 in the 1.5J/cm^2 profile (melt depth of 62nm and Sn level of 6E20/cm^3). This drop in Sn level could explain the disappearance of the XRD 2nd Ge peak in Fig.12b.

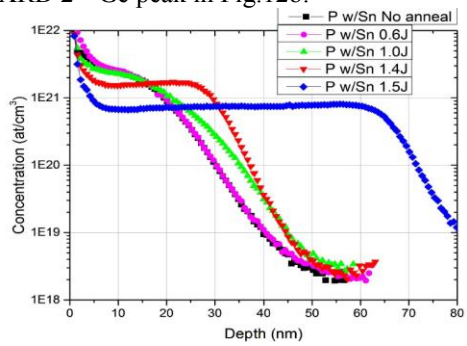

Fig.5: P SIMS for Sn+P implant region with 0.0, 0.6, 1.0, 1.4 and 1.5J/cm^2 laser anneal conditions.

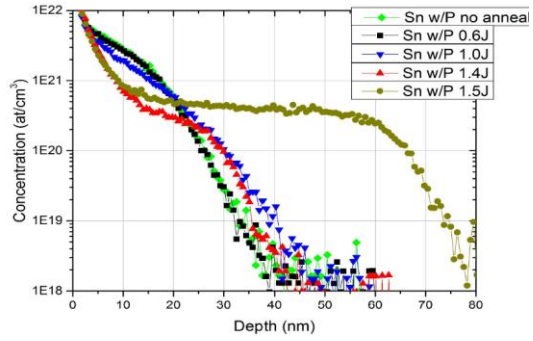

Fig.6: Sn SIMS depth profiles for the Sn+P implant region comparing no annealed up to 1.5J/cm^2.

The Sb SIMS results are shown in Fig.7 with an as implanted Xj of 26nm and the melt box-like profiles starting at 1.0J/cm^2 to a depth of 15nm (Xj=32nm) and 29nm at 1.4J/cm^2 (Xj=38nm).

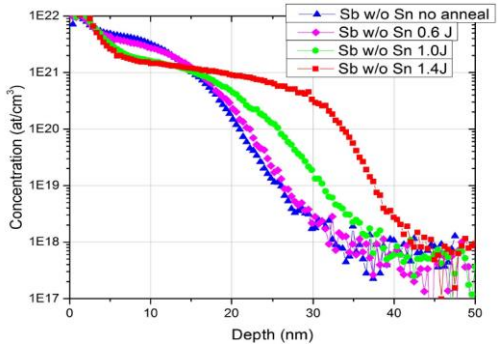

Fig.7: Sb SMS profiles for 0.0, 0.6, 1.0 and 1.4J/cm^2 laser anneal conditions.

Sb profiles for the Sn+Sb implant region is shown in Fig.8. The as implanted Sb Xj is now much deeper at 38.9nm with a retrograde surface profile. A slight change at 0.6J/cm^2 but at 1.0J/cm^2 a well-defined melt box-like profile to 28nm (Xj=45nm) with Sb pile-up at the surface. At 1.4J/cm^2 melt depth was 55nm and Xj=68nm. The Sn SIMS profiles are shown in Fig.9 with a slight retrograde profile compared to Fig.6 which has no retrograde Sn profile. Sn melt depth at 1.0J/cm^2 is 28nm and at 1.4J/cm^2 is 57nm.

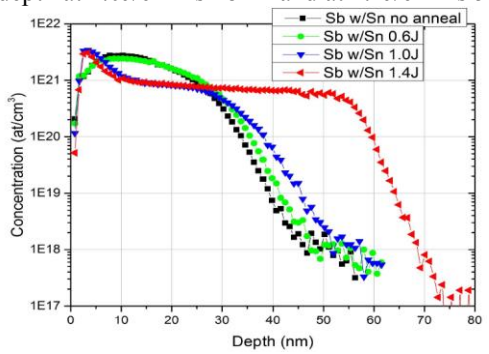

Fig.8: Sb SIMS profiles comparing Sn+Sb implant region for no anneal up to 1.4J/cm^2.

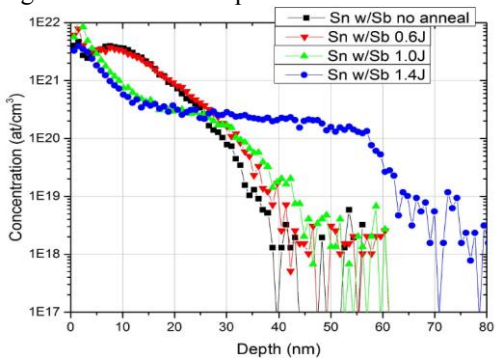

Fig.9: Sn SIMS profiles comparing Sn+Sb implant region for no anneal up to 1.4J/cm^2.

Using the Rs values from Fig.2 and the SIMS Xj values the updated Rs versus Xj chart is shown in Fig.10 for "this work" in comparison to others. P achieved ~2E20/cm^3 activation level for Xj=45-63nm when the melt depth exceeded the as implanted junction depth. Sb achieved the best ever reported n+ USJ activation level in Ge of ~8E20/cm^3 for Xj=38nm, 4x higher than P. Differential hall (DH) depth analysis also measures the surface n+ Rs depth profiles as shown in Fig.11 for P implant region. Rs was 600Ω/□ at Xj=10nm, 200Ω/□ at Xj=20nm and 65Ω/□ at Xj=45nm for a P activation level of 3-5E20/cm^3.

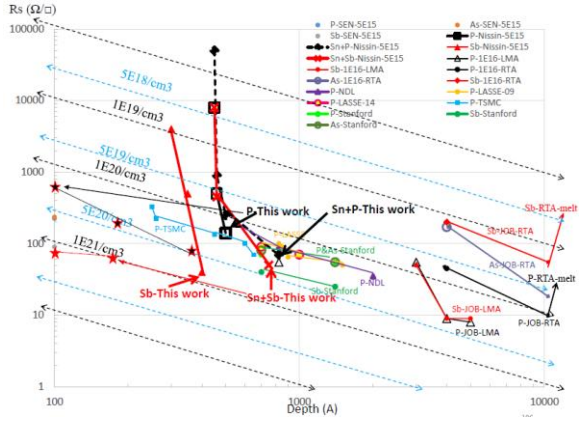

Fig.10: Rs sheet resistance versus n+ junction depth.

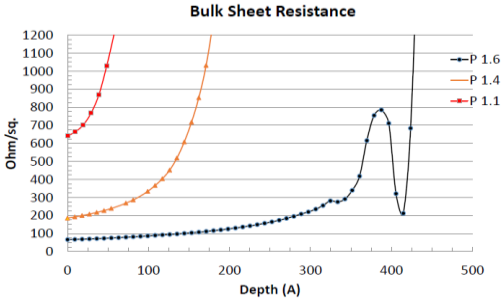

Fig.11: Differential Hall P-Rs n+ depth profiles.

XRD Strain-Ge Analysis

XRD strain-Ge analysis was provided by CNSE no shift in the Ge peak was seen for the P only and Sn+Sb implanted samples. However, a shift in the Ge peak to the left for the Sb only implant regions as the laser annealing energy density increases as shown in Fig.12a suggesting Ge surface tensile strain due to the larger substitutional Sb atom. The Sn+P implanted regions showed a 2nd peak to the right of the Ge peak in Fig.12b suggesting Ge surface compressive strain which is surprising since Sn atom is larger than Ge while P atom is smaller. This 2nd Ge peak disappeared when the Sn content level dropped from 3E21/cm^3 to <4E20/cm^3 when the laser anneal energy density went above 1.2J/cm^2 in the SIMS profile of Fig.6 with the drop in Sn areal density by 10x to 4E14/cm^2 at 1.4J/cm^2 but at 1.5J/cm^2 it recovered back up to 5E15/cm^2 with a surface of 6E20/cm^3.

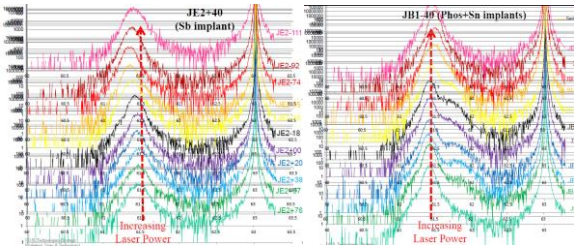

a) b)

Fig.12: XRD strain-Ge analysis for a) Sb and b) Sn+P implant regions with increasing laser energy density.

Differential Hall Mobility and Carrier Density Depth Profiles

ALP provided differential hall (DH) depth measurements for mobility, sheet resistance and dose analysis. Fig.13 shows the electron mobility results for P and Sb dopants at 1.1, 1.4 and 1.6J/cm^2 laser energy density anneals. P electron mobility remains flat at 72cm^2/V-s for 1.1J/cm^2, 76cm^2/V-s at 1.4J/cm^2 and 62cm^2/V-s at 1.6J/cm^2 laser anneal while Sb electron mobility degrades from 85cm^2/V-s at 1.1J/cm^2 to 42cm^2/V-s at 1.4J/cm^2 correlating to the XRD Ge peak shift to the left in Fig.12a. Adding Sn implant to P degraded electron mobility to 23cm^2/V-s at 1.1J/cm^2 but recovers to 68cm^2/V-s at 1.4J/cm^2 and 71cm^2/V-s at 1.6J/cm^2 laser anneals as the XRD 2nd Ge peak in Fig.12b disappears. Sn implant in Sb improved electron mobility by 2x to 144cm^2/V-s at 1.1J/cm^2, 116cm^2/V-s at 1.4J/cm^2 and 69cm^2/V-s at 1.6J/cm^2.

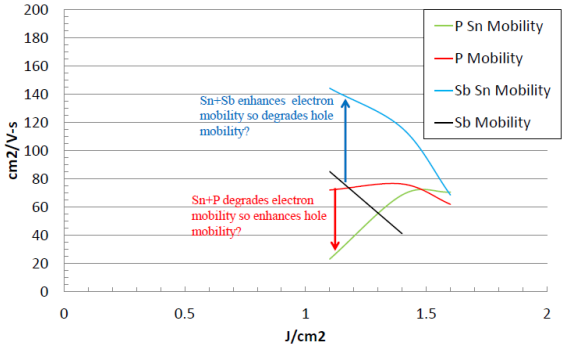

Figs.13: Electron mobility versus laser energy density.

Figs.14 and 15 shows DH layer mobility depth plots for the P, Sn+P, Sb and Sn+Sb samples. The results are different from bulk hall mobility where the depth component of strain-Ge can be significant especially for the Sn+Sb case where Sn creates a more uniform high electron mobility region in the top 30nm in Fig.15.

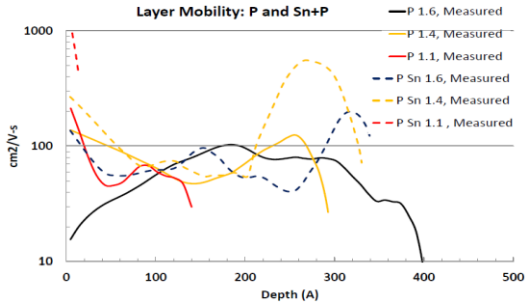

Fig.14: D-Hall layer mobility for P and Sn+P.

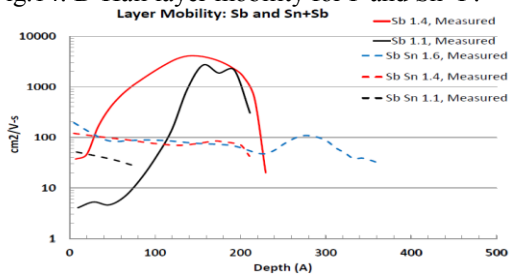

Fig.15: D-Hall layer mobility for Sb and Sn+Sb.

4. Conclusions

Ultra-shallow n+ ion implanted junctions with high dopant activation in high mobility thin Ge epilayer was realized by rapid and controlled Ge melt depth using 308nm Excimer laser annealing. Extremely high Sb activation of 1E21/cm^3 for 10nm USJ is >3x higher than best P activation level of 3E20/cm^3 for a 10nm USJ. High level of surface Sb also induced surface tensile strain-Ge which degraded electron mobility while Sn induced surface compressive strain-Ge improving Sb electron mobility by 2x but degraded P electron mobility by 3x. Differential Hall layer mobility depth plots shows Sn implant improved the mobility uniformity in the top 30nm surface. Controlled Ge melt depth can be extended to 7nm n+ USJ using sub-keV ultra-low energy implantation and results will be shown in the future with n+ activation of 1E21/cm^3.

References

[1] J. Borland and P. Konkola, IIT-2014, p.43-46.
[2] YJ Lee et al., IEDM-2012, paper 23.3, p.513.
[3] Mazzocchi et al., IEEE-RTP 2009, paper 21.
[4] Thareja et al., IEDM-2010, paper 10.5, p.245.
[5] Borland et al., IWJT 2013, paper S4-4, p.49-53.
[6] Borland et al., ECS Oct 2014, paper P7-1771, the Electrochemical Society, ECS Transactions, 64 (6), 127-145, (2014).
[7] Zaima et al, ECS Oct 2014, paper P7-1772, the Electrochemical Society, ECS Transactions, 64 (6), 147-153, (2014).